Electron-induced interaction of selected hydrocarbons with TiO_2 surfaces: the relevance to extreme ultraviolet lithography

2010 J. Phys.: Condens. Matter 22 084004

(http://iopscience.iop.org/0953-8984/22/8/084004)

J. Phys.: Condens. Matter **22** (2010) 084004 (8pp) doi:10.1088/0953-8984/22/8/084004

Electron-induced interaction of selected hydrocarbons with TiO_2 surfaces: the relevance to extreme ultraviolet lithography

B V Yakshinskiy[1,3], S Zalkind[1], R A Bartynski[1] and R Caudillo[2]

[1] Department of Physics and Astronomy, and Laboratory for Surface Modification, Rutgers, The State University of New Jersey, Piscataway, NJ 08854, USA
[2] Intel Corporation, Hillsboro, OR 97124, USA

E-mail: yaksh@physics.rutgers.edu

Received 1 July 2009, in final form 10 August 2009
Published 4 February 2010
Online at stacks.iop.org/JPhysCM/22/084004

Abstract
The aim of this work is to characterize desorption induced by electronic transition processes that affect the reflectivity of TiO_2-capped multilayer mirrors used in extreme ultraviolet (EUV) lithography. A low energy electron beam is employed to mimic excitations initiated by EUV radiation. Temperature programmed desorption, x-ray photoelectron spectroscopy, and low energy ion scattering are used to analyze the surface reactions. Carbon film growth on the TiO_2(011) crystalline surface is measured during 10–100 eV electron bombardment in benzene or methyl methacrylate vapor over a wide range of pressures and temperatures near 300 K. Low energy secondary electrons excited by EUV photons contribute substantially to the carbon accumulation on clean TiO_2 cap layers. For benzene on clean TiO_2, secondary electron effects dominate in the initial stages of carbon accumulation, whereas for C-covered TiO_2, direct excitations appear to dominate. We report on the adsorption energy, the steady-state coverage of the molecules on the surface and the cross sections for electron-stimulated dissociation: all key parameters for understanding and modeling the processes relating to the EUV lithography mirrors.

(Some figures in this article are in colour only in the electronic version)

1. Introduction

Extreme ultraviolet lithography (EUVL), which uses 13.5 nm wavelength (92 eV) radiation originating from plasma-based sources, is a leading technology for next generation semiconductor device manufacturing. Desorption induced by electronic transition (DIET) processes play important roles in the photoresist activation mechanisms. However, the lifetimes of reflection optics (i.e., the Mo/Si multilayer mirrors used for focusing EUV radiation) can be affected by oxidation or carbon accumulation due to radiation-induced surface chemistry in the inevitable background pressure of water vapor and hydrocarbons. Mirror lifetimes can be extended substantially by choice of appropriate cap layer materials. Promising cap layers for EUV applications include thin films (∼2 nm) of Ru, or TiO_2 [1, 2].

In our previous studies, to examine the effects of irradiation on the accumulation of C on model single-crystal Ru surfaces, we have bombarded the surfaces with low energy electrons (substitutes for EUV photons) while exposing them to methyl methacrylate (MMA, $C_5H_8O_2$) vapor, a model hydrocarbon outgassing product, and characterized the C film formation [3–6].

Recently, we have reported on contamination and mitigation of TiO_2(011) surface as a model capping layer [7, 8]. Bombardment of a crystalline TiO_2(011) surface by electrons with energies >25 eV causes desorption of O and O^+, creating a surface with oxygen vacancies that are

[3] Author to whom any correspondence should be addressed.

quantified using x-ray photoelectron spectroscopy (XPS). Via a similar mechanism, EUV photons can induce O-vacancies by direct core level ionization of TiO_2. The presence of O-vacancies accelerates the surface reactivity towards both thermal and non-thermal interactions with MMA and benzene.

In the present work, we expand the previous results for the important cases of benzene/TiO_2 and MMA/TiO_2. We focus on the accumulation of C on a TiO_2 surface for both thermal and non-thermal excitations; for non-thermal processes, we use electrons as substitutes for photons. Our argument is that most of the EUV-induced chemistry is caused by low energy secondary electrons photoemitted from the substrate, rather than direct photon-excitation of adsorbates [9]. Benzene (C_6H_6) and MMA are models for the hydrocarbon background gases that arise from resist outgassing in a typical EUVL vacuum chamber. First, we show the importance of such parameters as the surface temperature, hydrocarbon pressure and energy of bombarding electrons for irradiation-induced growth of carbon. Increasing the substrate temperature lowers the carbon accumulation rate, increasing the vapor pressure enhances the carbon deposition, and variation of the electron energy shows a pronounce influence on the reaction rate. Then, we characterize the adsorption/desorption behavior of benzene and MMA on clean and C-covered $TiO_2(011)$, measure the adsorption energies and estimate the sticking probabilities. After that we present the hydrocarbon equilibrium coverage as a function of pressure and temperature. Finally, we describe experiments to determine the cross sections for electron-induced dissociation of benzene and MMA on clean and C-covered TiO_2. These parameters (adsorption energies, sticking probabilities, magnitude and electron energy dependence of dissociation cross sections, etc) will provide key data for modelers of EUV contamination rates.

2. Experimental procedures

The measurements are made in a stainless-steel ultrahigh vacuum chamber with a base pressure $<1 \times 10^{-10}$ Torr containing instrumentation for a variety of surface science characterization tools [10]. The surface chemical composition of the topmost layer of the sample is estimated using low energy He^+ ion scattering (LEIS) and the near surface composition is determined using x-ray photoelectron spectroscopy (XPS), mainly for grazing emission (30°) to maximize surface sensitivity. Scattered ions and photoemitted electrons are energy-analyzed using a 100 mm radius concentric hemispherical analyzer. A tunable low energy electron source (0–200 eV) is used to initiate electron-stimulated surface reactions and molecular decomposition [11].

The rutile $TiO_2(011)$ single crystal ($10 \times 10 \times 0.5$ mm^3, MTI, Inc.) is mounted on an X–Y–Z rotary manipulator that can be cooled by liquid nitrogen to ∼110 K and resistively heated to >1500 K. We have chosen $TiO_2(011)$ face of titania due to its unusual behavior, in particular, the self-organization of O-vacancies on the (2×1) termination of $TiO_2(011)$ under electron irradiation [12]. Cleaning of surface is accomplished by a combination of 1 keV Ar ion bombardment and annealing in oxygen at a pressure of 10^{-7} Torr. Temperature programmed desorption (TPD) is used to measure desorption temperature and binding energy of the adsorbates as well as the surface coverage. To optimize thermal contact for TPD from TiO_2, the sample is mounted onto a thin Ti heating plate through a gold foil that insures uniform heating. The temperature was measured using a chromel–alumel thermocouple spot welded to the rear side of the sample assembly. As the surface is heated at a linear rate, the desorbing atoms are detected using a quadrupole mass spectrometer (QMS).

To examine the effects of electron irradiation on the buildup of C on the TiO_2 surface, we have bombarded the entire sample with a defocused electron beam while exposing it to a hydrocarbon vapor from a capillary array doser. Carbon film thicknesses during accumulation under electron bombardment in the presence of hydrocarbon vapor are mainly determined by measurements of the Ti 2p peak attenuation. But within submonolayer range the estimation of the amount of carbon is based on the measurement of the C 1s peak intensity. Pressures of MMA and benzene are measured using an uncalibrated Bayard–Alpert ionization gauge, and the pressures reported here are local pressures at the sample surface, corrected for the factor ∼10× enhancement of the doser.

3. Results and discussion

3.1. Electron-stimulated growth of carbon under MMA and benzene atmosphere

In order to evaluate the parameters that govern the carbon accumulation under electron irradiation and exposure to MMA and benzene, we examined the substrate temperature, the hydrocarbon pressure and electron energy dependences of the carbon deposition rate.

Figure 1 presents carbon film growth on the TiO_2 surface as a function of the electron irradiation dose, for different substrate temperatures in (a) MMA and (b) benzene atmospheres. It can be seen that for MMA exposure after the initial similar carbon growth, and for benzene throughout the entire growth process, increasing the substrate temperature lowers the carbon accumulation rate. This decrease occurs due primarily to the drop of residence time and adsorbate surface concentration at elevated temperatures. The initial growth rate is higher on the clean surface, declining toward a constant growth rate on the carbon covered surface. This will be discussed later in conjunction with the steady-state coverages of MMA and benzene on the surface and the electron-induced reaction cross section for these molecules on the clean and carbon covered surfaces. It can be also seen that for the same conditions, the carbon deposition rate from MMA vapor is roughly twice as high as that from benzene vapor.

The influence of the hydrocarbon vapor pressure on the carbon growth rate at room temperature is shown in figure 2. It is not surprising that increasing the vapor pressure over the surface enhances the carbon deposition.

In our experiments we are using low energy electrons, in the energy range up to 100 eV, to mimic the reaction of the 92 eV (13.5 nm) photons in the EUVL apparatus. The

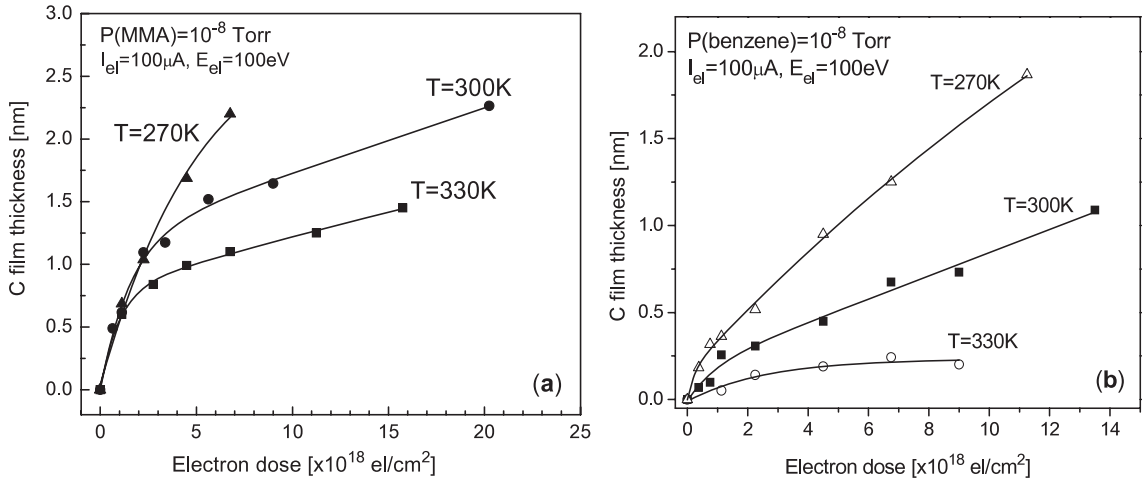

Figure 1. The influence of substrate temperature on carbon growth as a function of electron irradiation dose: (a) during exposure to MMA, (b) during exposure to benzene. The carbon thickness is calculated from attenuation of the Ti 2p XPS signal.

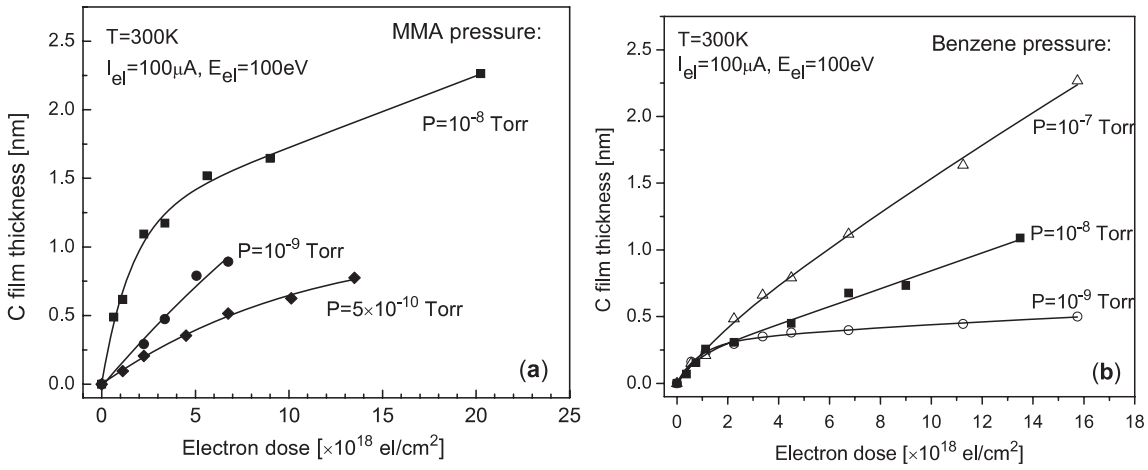

Figure 2. The influence of vapor pressure on carbon growth as a function of electron irradiation dose: (a) in MMA atmosphere, (b) in benzene atmosphere. The carbon thickness is calculated from attenuation of the Ti 2p XPS signal.

photons can be absorbed directly by the adsorbed hydrocarbon molecules on the surface [9] or can generate low energy secondary electrons that are ejected from the surface and can cause dissociation of surface molecules [2, 7]. Figure 3 illustrates the irradiation-induced carbon film growth from benzene vapor for two electron energies and shows the pronounce influence of electron energy on the reaction rate.

The above results indicate the importance of such parameters as temperature, pressure and electron energy. In the following sections we will try to give an insight how these parameters affect the reaction with MMA and benzene layers and carbon accumulation.

3.2. TPD measurements of MMA and benzene from clean and carbon covered surfaces

To estimate the desorption energies of MMA and benzene from clean and carbon covered TiO_2 surface, sequential TPD measurements were performed for increasing doses. All hydrocarbon exposures are done at the substrate temperature of 110 K. A series of TPD spectra for various MMA doses on the clean TiO_2 surface is shown in figure 4.

For the monolayer saturated MMA coverage, the desorption peak maximum corresponds to ∼180 K, and the shift in the TPD spectra to lower temperatures indicates that the adsorption energy decreases monotonically with increasing coverage. The inset in figure 4 shows the dependence of TPD peak area versus MMA exposure. Although this uptake curve passes through the origin, which basically indicates that the MMA desorbs without dissociation, it is notable that the curve is also somewhat concave. The nonlinear behavior of the uptake curve implies that some minor fraction of the MMA dissociates and thermally reacts with the TiO_2 surface, probably with the surface defects. The XPS analysis performed after a few adsorption–desorption cycles showed a slight increase in the C 1s intensity over the background level, which indicates some thermal dissociation and carbon accumulation on the surface. When the surface defects are blocked with carbon, the MMA decomposition reduces and therefore an increase in the slope of uptake curve is observed. A similar

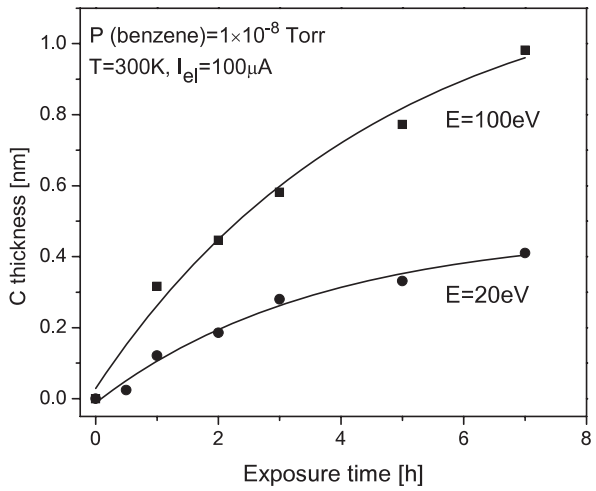

Figure 3. The influence of electron energy on the irradiation-induced carbon growth on TiO_2 in benzene atmosphere as a function of exposure time.

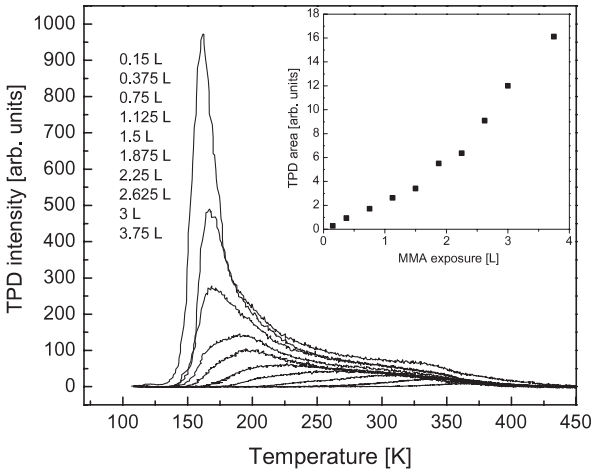

Figure 4. TPD of MMA from clean TiO_2. The inset shows the uptake curve which slightly concave shape indicates some dissociation and carbon accumulation on the surface, probably, on surface defects.

change of the uptake curve slope was also found for MMA reaction with Ru surface [5]. The increasing MMA uptake with MMA exposure can also be explained by the increasing sticking coefficient with coverage over the transition from the first to the second ML of adsorbate.

A similar set of TPD spectra for progressive benzene doses on clean TiO_2 surface is shown in figure 5. Since the adsorption energy scales with peak temperature, this implies that the adsorption energy decreases as adsorbate coverage increases. For the ∼1 ML saturated benzene coverage, the maximum desorption rate is positioned at ∼170 K. As the coverage increases further, a second peak develops at ∼150 K that we identify as the onset of multilayer formation for both benzene and MMA (figure 4). The linear shape of the uptake curve (inset in figure 5) is evidence of a constant sticking probability and the absence of carbon accumulation during the TPD of benzene from clean TiO_2. It can be seen that the temperature corresponding to the maximum in the desorption rate at low MMA coverage (figure 4) is relatively high, above

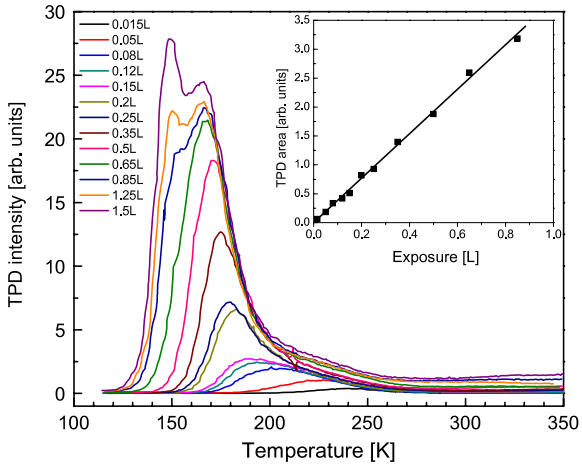

Figure 5. TPD of benzene from clean TiO_2. The inset shows the uptake curve (TPD peak area versus exposure).

room temperature, in contrast to desorption peak position for benzene, which has a low coverage maximum at ∼250 K.

For the experiments related to the figures 6 and 7 the carbon covered surface was prepared by the electron irradiation of the TiO_2 sample surface at room temperature with the dose of $\sim 2 \times 10^{19}$ el cm^{-2} in the presence of MMA vapor at pressure $\sim 10^{-8}$ Torr (see figures 1 and 2). Figure 6 presents TPD spectra for MMA from ∼2.2 nm thick carbon covered surface for high (figure 6(a)) and low (figure 6(b)) MMA exposures. A continuous shift of desorption peak towards lower temperatures can also be seen, similar to desorption from the clean surface (figure 4), although the desorption temperatures, especially for the initial coverage, are significantly lower. The uptake curve is linear and passes through the origin, which indicates a constant sticking probability and total reversible desorption of the MMA molecules.

Figure 7 illustrates the TPD of benzene from C-covered TiO_2 sample. Note that in this case, as well as for MMA desorption (figure 6), we see no clear evidence for a second peak, indicating the single ML and multilayer peaks overlap on the surface. The nonlinear uptake curve (inset in figure 7) indicates that the sticking probability is coverage dependent and decreases with coverage growth. The absence of the single ML can also be explained by the non-wetting adsorption on the carbonized surface. Nonetheless, the fact that the uptake curves pass through the origin in both inset plots of figures 5 and 7 is evidence that benzene adsorbs and desorbs reversibly, without dissociation. This is consistent with previous reports on benzene non-dissociative adsorption on TiO_2 [13–17].

Assuming first order kinetic for the MMA desorption (the molecule adsorbs and desorbs without dissociation–recombination) we exploited simple Redhead equation containing relationship between the peak temperature and the binding energy [18, 19], to estimate the adsorption energies at low coverage.

Figure 8 shows the calculated adsorption energies for low coverage of MMA and benzene on clean and carbon covered surfaces. The extrapolation of adsorption energy to zero

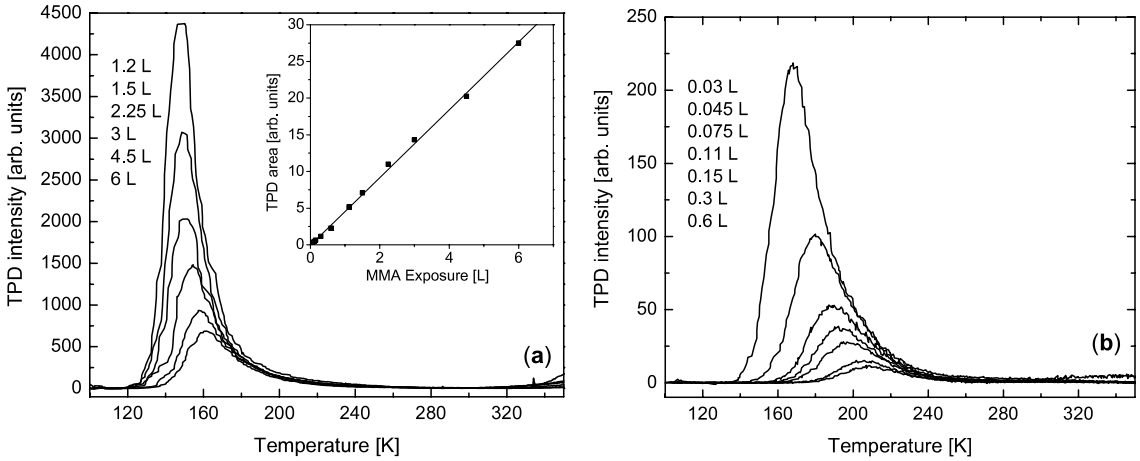

Figure 6. TPD of MMA from 2.2 nm carbon covered TiO_2. For better presentation, the curves are divided into two groups: (a) high and (b) low coverage. The inset represents the uptake curve.

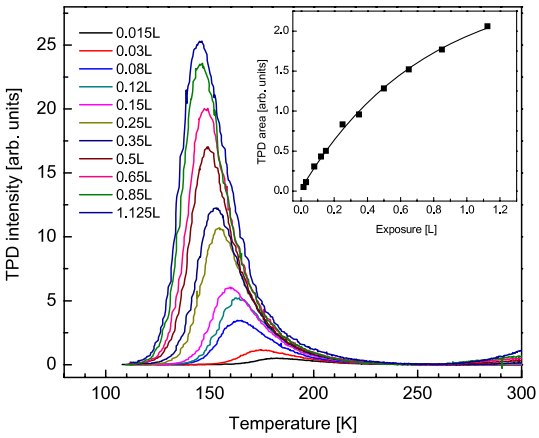

Figure 7. TPD of benzene from 2 nm carbon covered TiO_2. The inset represents the uptake curve.

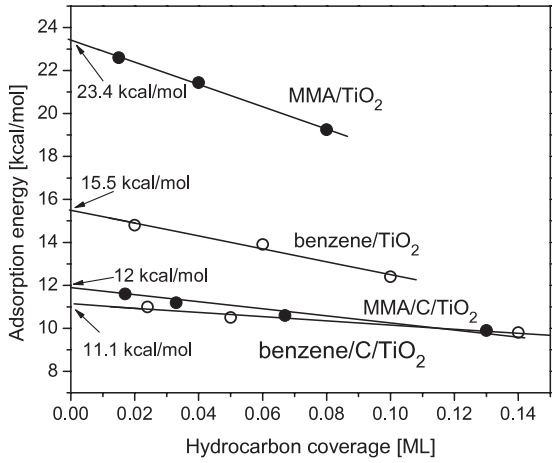

Figure 8. Low coverage adsorption energy of MMA and benzene on clean and C-covered surfaces, as extracted from TPD results (figures 4–7). The extrapolation to zero coverage adsorption energy is indicated.

coverage value is shown. The low coverage adsorption energy results for benzene and MMA are in good agreement with those found for benzene adsorption on TiO_2 [16] and ZnO [20] and for MMA on Ru [6].

3.3. Steady-state coverages of MMA and benzene on the surface

One of the parameters that strongly influences the irradiation-induced reaction rates is the adsorbate concentration on the surface during photon/electron bombardment. To estimate the steady-state adsorbate coverage on the surface under a given pressure of benzene or MMA (isobaric conditions) we exploit two techniques: TPD for the low pressure regime (10^{-10}–10^{-8} Torr), and LEIS for the higher pressure range ($<10^{-6}$ Torr), as described in details previously [8]. In brief, during the TPD measurements the sample was placed in front of the QMS aperture and kept at the desired temperature (300 and 340 K). The chamber was backfilled to the indicated gas pressure and after establishing equilibrium conditions on the surface, the sample was heated and a TPD spectrum was recorded. By comparing the TPD intensities with those obtained from regular TPD, the coverage of adsorbed molecules at the indicated pressure can be deduced. To evaluate the steady-state coverage on clean TiO_2 at the higher pressure range we used the attenuation of the titanium and oxygen signals in the LEIS spectrum under the given gas pressure.

Figure 9 shows the low pressure benzene steady-state coverage, obtained by TPD, plotted versus log p for benzene on the clean and carbon covered TiO_2 surfaces at 300 and 340 K.

Figure 10 represents the low pressure MMA steady-state coverage, obtained by TPD, plotted versus log p for MMA on the clean and carbon covered TiO_2 surfaces at 300 K.

The steady-state coverage for benzene and MMA in the higher pressure range (5×10^{-9}–5×10^{-7} Torr) on clean TiO_2 as a function of log p, obtained by LEIS, is presented in figure 11. The concentrations of benzene and MMA are higher on the clean TiO_2, than on the carbon covered surface. The coverage of the MMA is higher than benzene coverage

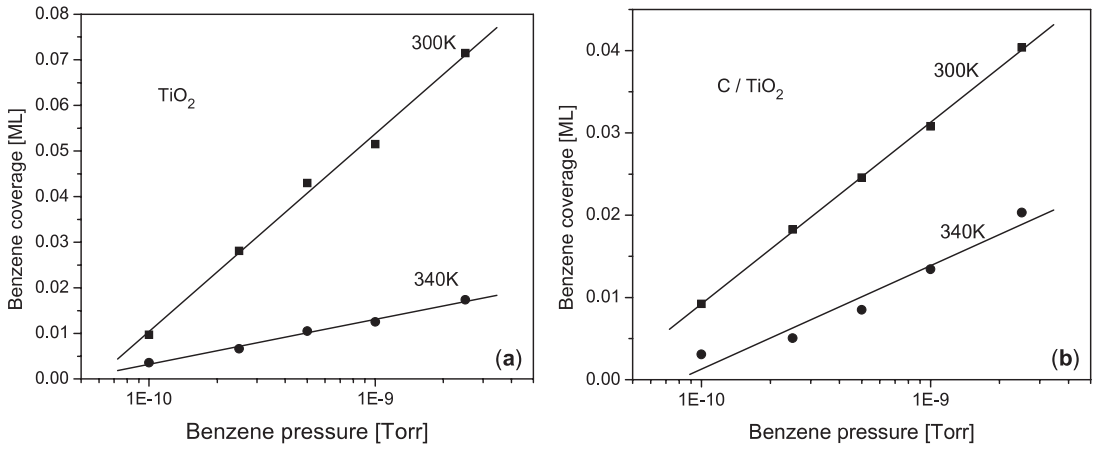

Figure 9. Steady-state benzene coverage for low pressure range, obtained from isobaric TPD measurements at the sample temperatures of 300 and 340 K on (a) clean and (b) carbon covered TiO_2 surfaces.

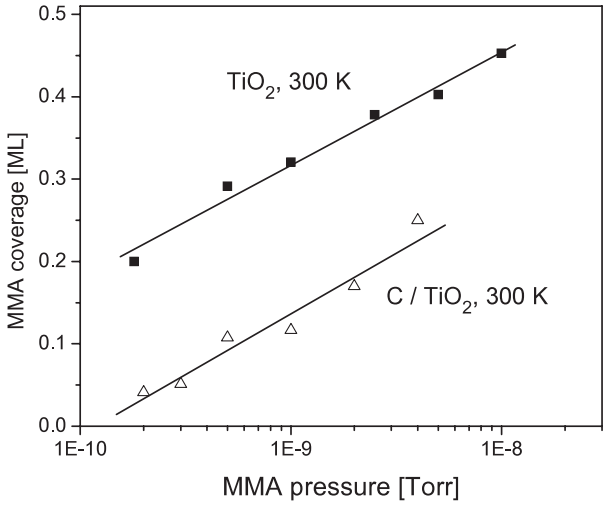

Figure 10. Steady-state MMA coverage for low pressure range, obtained from isobaric TPD measurements at the sample temperature of 300 K on clean and carbon covered TiO_2 surfaces.

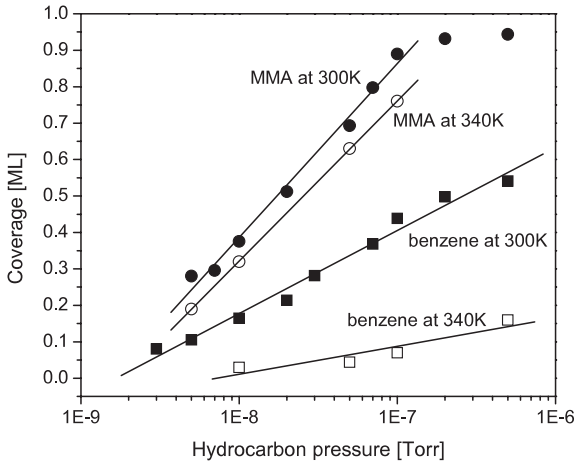

Figure 11. High pressure steady-state MMA and benzene coverage on clean TiO_2, as obtained from LEIS measurements at the sample temperature of 300 and 340 K.

and reaches ∼90% ML at a pressure of 2×10^{-7} Torr. It is also clear that temperature has a reversible effect on the steady-state coverage for both gases.

It is worthwhile to note that the coverage depends linearly on the logarithm of benzene and MMA pressure, $\log p$. As discussed in [7], for simple adsorption kinetics (equivalent surface sites, non-dissociative adsorption, first order desorption, constant adsorption energy per site independent of coverage), the functional relation between steady-state coverage Θ and the pressure p is given by the Langmuir adsorption isotherm [18]. In this case, the steady-state coverage Θ is proportional to p in the low coverage limit. The fact that in our case Θ is proportional to $\log p$ indicates that the adsorption energy is not constant and depends on coverage. This functional form is consistent with the Temkin adsorption isotherm [18]. The Temkin adsorption isotherm is based on the assumption that the adsorption energy E decreases linearly with increasing coverage due to repulsive lateral interactions, as $E = E_o(1 - a\Theta)$, where E_o and a are constants. Such a linear dependence of adsorption energy on coverage is consistent with the data shown in figure 6, for benzene and MMA adsorption energies.

3.4. Measurements of cross section for electron-induced reaction with benzene and MMA layers

As one can see in figure 3, the energy of the incident electrons affects the carbon accumulation rate on the surface. Therefore, characterization of this energy dependence and cross section measurements of the reaction of electrons with benzene and MMA layers is of great importance for modeling the carbon growth reaction. The change of the surface concentration of the adsorbed species due to radiation can be expressed as

$$-\frac{\mathrm{d}N}{\mathrm{d}t} = n\sigma N, \tag{1}$$

where N is the density of adsorbed species, t is the time, n is the electron flux ($\mathrm{cm}^{-2}\ \mathrm{s}^{-1}$) and σ is the total cross section for dissociation/desorption (cm^2) due to irradiation. The cross section measurements were performed on clean and on carbon covered surface for different electron energies. Figure 12

Table 1. Total cross sections of electron-induced reactions for MMA and benzene on clean and carbon covered TiO_2 surfaces at different electron energies.

Electron energy (eV)	MMA/TiO_2 cross section (cm^2)	MMA/C/TiO_2 cross section (cm^2)	Benzene/TiO_2 cross section (cm^2)	Benzene/C/TiO_2 cross section (cm^2)
10	1.6×10^{-17}	1.5×10^{-17}	3.5×10^{-17}	
20	3.8×10^{-17}	1.9×10^{-17}	8.1×10^{-17}	4×10^{-18}
50	6.1×10^{-17}	5.2×10^{-17}		6×10^{-18}
100	1.1×10^{-16}	7×10^{-17}	1.3×10^{-16}	1.3×10^{-17}

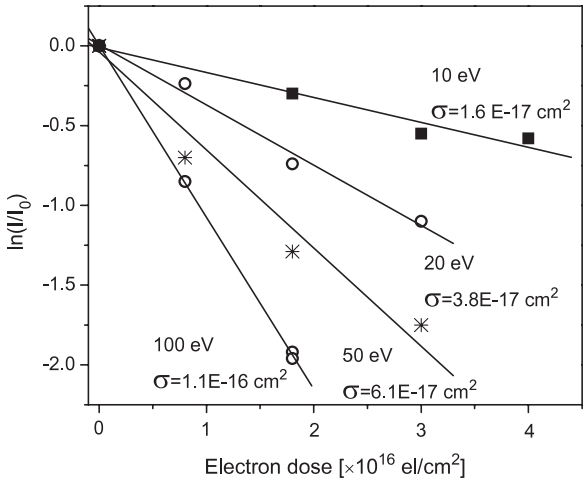

Figure 12. Measurement of cross sections for different electron energy reactions with 1 ML of MMA on clean TiO_2 surface. I_0—the TPD peak area for 1 ML of MMA desorption, and I—the TPD peak area corresponding to desorption of intact fraction of ML of MMA.

illustrates the cross section measurements by TPD of unreacted part of adsorbate for electron-induced reaction in 1 ML of MMA on TiO_2. Here I_0 is the TPD peak area, corresponding to 1 ML of adsorbate, and I is the TPD peak area corresponding to intact, unreacted fraction of ML of MMA.

Table 1 summarizes the total cross section data.

Electron interaction with the adsorbed molecules can cause desorption from the surface, as well as dissociation and transform of adsorbed molecules into residual carbon on the surface. Since the latter is of interest here, these two phenomena have to be distinguished. The amount of residual carbon can be evaluated by comparing the C 1s XPS intensity of the residual carbon after electron irradiation and TPD with the carbon intensity for the initial adsorbed monolayer, as shown in figure 13 for 100 eV electron bombardment. Here I_0—integrated C 1s intensity corresponding to the initial organic ML (MMA or benzene), and I—integrated C 1s intensity corresponding to the carbon as a product of electron-stimulated reaction after removal of unreacted fraction of the adsorbate. About 0.7 of the initial MMA layer and 0.3 of the initial benzene layer are transformed into carbon, while the rest desorbs during irradiation.

4. Summary and conclusions

A key issue in EUV mirror contamination concerns the mechanisms by which mirror cap layers become oxidized or carbon covered during EUVL. The following are the relative contributions of direct photoexcitation and indirect excitations via low energy secondary electrons. Our experiments for benzene provide evidence that low energy secondary electrons play a major role in carbon accumulation on clean TiO_2. Consider the ratio E/P of the number of hydrocarbon molecules dissociated by secondary electrons (E) to the number of molecules that are dissociated by primary photons (P). Taking into account the cross section for carbon accumulation under 10 eV electron irradiation, resonance

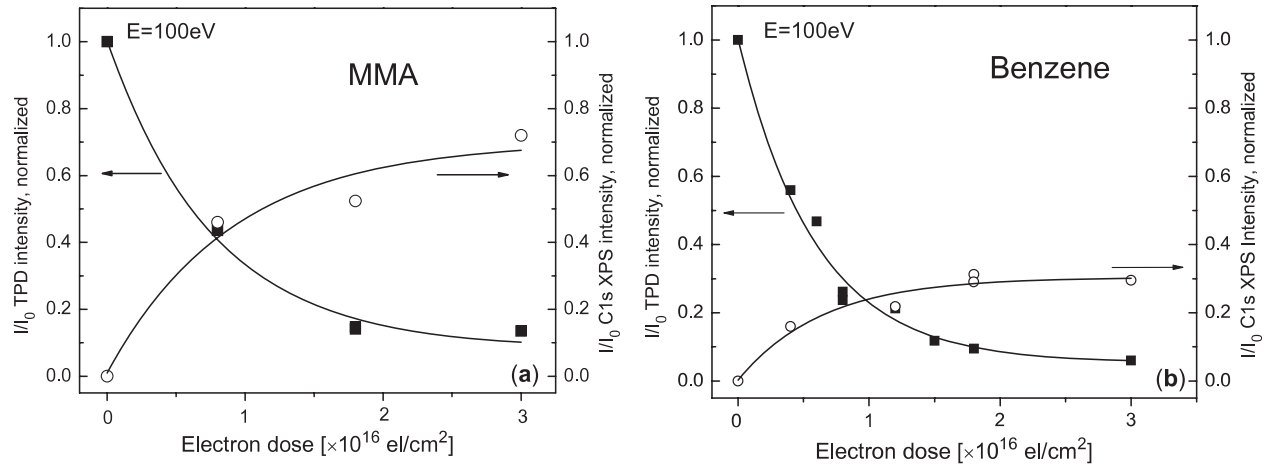

Figure 13. The right axes: ratio between C 1s XPS intensity I for the residual carbon after electron irradiation and TPD and C 1s intensity I_0 for the initial adsorbed (a) MMA and (b) benzene monolayers. The left axes: complimentary TPD results, where I and I_0 represent the TPD intensities for unreacted fraction of monolayer and 1 ML of adsorbate, respectively.

effects due to the TiO_2-capped MLM structure [21], substrate quenching effects, our value of the ratio yields E/P $\approx$ 1 [8]. This is in contrast with a model reported by Hollenshead and Klebanoff [9], where the maximal value E/P is about a factor 50 times smaller. A similar analysis for the benzene on C-covered TiO_2 yields E/P $\approx$ 0.1 i.e. as the surface becomes covered with carbon suggests that the subsequent growth rate is dominated by direct (EUV) photon excitations.

These analyses imply that the relative contributions of direct photoexcitations and indirect (secondary electron) excitations in carbon accumulation on EUVL cap layers must be considered on a case-by-case basis. They will differ for various gases and cap layer materials. The relative contributions will depend on the background gas composition, the magnitudes of cross sections for indirect excitations, the composition of the cap layer, and the resonant enhancement of secondary electron yields for the capped MLM.

In this paper we also reported on the adsorption energy and steady-sate coverage of benzene and MMA on the clean and carbon covered TiO_2 surface. It was found that the coverage depends on the log of gas pressure. According to the Temkin isotherm [18] this implies that the adsorption energy E decreases with increasing coverage due to repulsive lateral interactions. Depending on the pressure, the coverage of molecules on the surface can be significant, where for MMA the coverage reaches a limiting value high as $\sim$0.9 ML at 2×10^{-7} Torr. It seems therefore, that in an unbaked and organic-molecule-containing EUVL chamber, the coverage of those molecules on the surface can be significant, providing the building blocks for a carbon layer. The steady-state coverage of the molecules on the surface and the cross sections for reaction are key parameters for understanding and modeling the processes on the EUVL mirrors.

Acknowledgments

The authors thank Drs T Lucatorto, S Hill and N Faradzhev of NIST for valuable discussions. This work has been supported by the Intel Corporation.

References

[1] Bajt S, Edwards N V and Madey T E 2008 Properties of ultrathin films appropriate for optics capping layers exposed to high energy photon irradiation *Surf. Sci. Rep.* **63** 73–99

[2] Madey T E, Faradzhev N S, Yakshinskiy B V and Edwards N V 2006 Surface phenomena related to mirror degradation in extreme ultraviolet (EUV) lithography *Appl. Surf. Sci.* **253** 1691–708

[3] Yakshinskiy B V, Wasielewski R, Loginova E and Madey T E 2007 Carbon accumulation and mitigation processes, and secondary electron yields of ruthenium surfaces *Proc. SPIE* **6517** 65172Z

[4] Yakshinskiy B V, Wasielewski R, Loginova E, Hedhili M N and Madey T E 2008 DIET processes on ruthenium surfaces related to extreme ultraviolet lithography (EUVL) *Surf. Sci.* **602** 3220–4

[5] Hedhili M N, Yakshinskiy B V, Wasielewski R, Ciszewski A and Madey T E 2008 Adsorption and electron-induced polymerization of methyl methacrylate on Ru (10-10) *J. Chem. Phys.* **128** 174704

[6] Wasielewski R, Yakshinskiy B V, Hedhili M N, Ciszewski A and Madey T E 2007 Surface chemistry of Ru: relevance to optics lifetime in EUVL *Proc. SPIE* **6533** 653316

[7] Yakshinskiy B V, Hedhili M N, Zalkind S, Chandhok M and Madey T E 2008 Radiation-induced defect formation and reactivity of model TiO_2 capping layers with MMA: a comparison with Ru *Proc. SPIE* **6921** 692114

[8] Zalkind S, Yakshinskiy B V and Madey T E 2008 Interaction of benzene with TiO_2 surfaces: relevance to contamination of extreme ultraviolet lithography mirror capping layers *J. Vac. Sci. Technol.* B **26** 2241–6

[9] Hollenshead J and Klebanoff L 2006 Modeling radiation-induced carbon contamination of extreme ultraviolet optics *J. Vac. Sci. Technol.* B **24** 64–82

[10] Yakshinskiy B V, Madey T E and Ageev V N 2000 Thermal desorption of sodium atoms from thin SiO_2 films *Surf. Rev. Lett.* **7** 75–87

[11] Lin J-L and Yates J T Jr 1994 Electron gun for producing a low energy, high current, and uniform flux electron beam *J. Vac. Sci. Technol.* A **12** 2795–7

[12] Dulub O, Batzill M, Solovev S, Loginova E, Alchagirov A, Madey T E and Diebold U 2007 Electron-induced oxygen desorption from the TiO_2(011)-2 $\times$ 1 surface leads to self-organized vacancies *Science* **317** 1052–6

[13] Diebold U 2003 The surface science of titanium dioxide *Surf. Sci. Rep.* **48** 53–229

[14] Raza H, Wincott P L, Thornton G, Casanova R and Rodriguez A 1998 Photoemission studies of the reaction of benzene with TiO_2 (100) 1 $\times$ 1 and 1 $\times$ 3 *Surf. Sci.* **402–404** 710–4

[15] Suzuki S, Yamaguchi Y, Onishi H, Sasaki T, Fukui K and Iwasawa Y 1998 Study of pyridine and its derivatives adsorbed on TiO_2(110)-(1 $\times$ 1) surface by means of STM, TDS, XPS and MD calculation in relation to surface acid-base interaction *J. Chem. Soc. Faraday Trans.* **94** 161–6

[16] Reiß S, Krumm H, Niklewski A, Staemmler V and Wöll Ch 2002 The adsorption of acenes on rutile TiO_2(110): a multi-technique investigation *J. Chem. Phys.* **116** 7704–12

[17] Zhou J, Dag S, Senanayake S D, Hathorn B C, Kalinin S V, Meunier V, Mullins D R, Overbury S H and Baddorf A P 2006 Adsorption, desorption, and dissociation of benzene on TiO_2(110): experimental characterization and first-principles calculations *Phys. Rev.* B **74** 125318

[18] Masel R I 1996 *Principles of Adsorption and Reaction on Solid Surfaces* (New York: Wiley) chapter 4

[19] Redhead P A 1962 Thermal desorption of gases *Vacuum* **12** 203–11

[20] Pöss D, Ranke W and Jacobi K 1981 Adsorption and epitaxial growth of benzene on ZnO(10-10) studied by thermal desorption spectroscopy, LEED and UPS *Surf. Sci.* **105** 77–94

[21] Hill S B, Faradzhev N S, Tarrio C, Lucatorto T B, Madey T E, Yakshinskiy B V, Loginova E M and Yulin S 2008 Accelerated lifetime metrology of EUV multilayer mirrors in hydrocarbon environments *Proc. SPIE* **6921** 692117